INTERNATIONAL JOURNAL FOR NUMERICAL METHODS IN FLUIDS, VOL. 11, 397–404 (1990)

FINITE ELEMENT ANALYSIS OF CREEPING FLOWS USING MARKER PARTICLES

TAKEO SHIOJIMA
Idemitsu Petrochemical Co., Ltd., Chiba, Japan

YOJI SHIMAZAKI
Tokai University, Kanagawa, Japan

AND

HISAAKI DAIGUJI
Tohoku University, Miyagi, Japan

SUMMARY

The penalty function formulation of the finite element method is described for the analysis of transient incompressible creeping flows. Marker particles are utilized to represent moving free surfaces and to visualize the flow patterns. For determining the movement of markers from element to element, the area coordinate system of the linear triangular element is introduced.

With the method presented, a punch indentation problem and an injection problem for an L-shaped cavity are solved for Newtonian and power-law fluids.

KEY WORDS Numerical analysis Finite element method Transient flow Free surface flow Creeping flow Power-law fluid

1. INTRODUCTION

The analysis of time-dependent flows with deforming free surfaces is one of the most important areas in technological and engineering fields, such as those found in polymer injection mouldings. For analysing the flows numerically, several types of methods are now available.

The finite element method applied to these flow problems often incorporates the mesh-rezoning method,[1] in which the velocity calculated in the Lagrangian description is utilized for determining the new mesh arrangement. With this method, however, difficulties will arise if there are obstacles in the domain of the analysis. In order to avoid these difficulties, a method which interpolates a Lagrangian velocity into a Eulerian system can be used.[2] The disadvantage of this method is that the calculated shape of the free surfaces depends on the shape of the original mesh.

On the other hand, when using the finite difference method there are so-called MAC and PIC methods for analysing the flow.[4,5] These methods make use of marker particles to indicate free surfaces. The flow patterns can be visualized if the markers are also arranged inside the transient flow. These methods, however, are difficult to apply under complicated fixed boundary conditions. Such conditions can easily be covered if the finite element method is used.

In this study we present a finite element method for analysing transient incompressible creeping flows. Marker particles are used to represent free surfaces and to visualize flow patterns. The

0271–2091/90/120397–08$05.00

Received August 1988
Revised December 1989

penalty function formulation is used to solve the velocity field. The markers in a finite element can well simulate the deforming free surfaces simply by moving towards the direction of the velocity vectors. In order to move the markers to indicate the successive moving free surfaces, the area co-ordinate system of the linear triangular element, which is utilized for determining the new marker position in an element, is introduced into the four-node rectangular isoparametric element.

A punch indentation problem is first solved to verify the scheme and the results are compared with those obtained by the mesh-rezoning method. In the second example problem, successive stages of deforming free surfaces by the injection moulding of an L-shaped cavity are shown. Both power-law and Newtonian fluids are considered here.

2. GOVERNING EQUATIONS

We first present the general governing equations for the time-dependent creeping flows of incompressible Newtonian and power-law fluids in rectangular Cartesian co-ordinates. The equations without body forces are

equilibrium

$$-\rho u_{i,t} + \sigma_{ij,j} = 0, \tag{1}$$

continuity (incompressible fluids)

$$u_{i,i} = \varepsilon_{ii} = 0, \tag{2}$$

constitutive relationships

$$\sigma_{ij} = \sigma'_{ij} + p\delta_{ij}, \tag{3}$$

$$\varepsilon_{ij} = (u_{i,j} + u_{j,i})/2, \tag{4}$$

$$\sigma'_{ij} = 2\mu\varepsilon_{ij}, \tag{5}$$

$$\mu = \text{constant} \quad \text{(Newtonian fluids)}, \tag{6}$$

$$\mu = \mu_0(4I_2(\varepsilon))^{(n-1)/2} \quad \text{(power-law fluids)} \tag{7}$$

$$I_2(\varepsilon) = \varepsilon_{ij}\varepsilon_{ij}, \tag{8}$$

boundary conditions

$$u_i = \bar{u}_i \quad \text{on} \quad S_u, \tag{9}$$

$$\nu_j\sigma_{ij} = \bar{T}_i \quad \text{on} \quad S_t, \tag{10}$$

where ρ is the density, σ_{ij} is the total stress, σ'_{ij} is the deviatoric stress, p is the pressure, u_i is the velocity component in the x_i-direction, $\bar{u}_i$ is the specified velocity on S_u, $\bar{T}_i$ is the specified traction on S_t with unit outward normal vector ν_j, μ is the viscosity coefficient and μ_0 and n are the material constants.

3. NUMERICAL SCHEME

In order to obtain the solution for equations (1) and (2) we use the penalty function formulation of the finite element method,[6] and to obtain the positions of moving free surfaces, marker particles are utilized.

3.1. Finite element method for equations (1) and (2)

The velocity is interpolated as

$$u_i \simeq N_\alpha u_{\alpha i}, \tag{11}$$

where N_α is the shape function for the velocity and $u_{\alpha i}$ is the nodal velocity. Galerkin's method applied to equation (1), with the weighting functions chosen to be the same as the approximate function, gives

$$-\int_v \rho N_\alpha u_{i,t}\,dv + \int_v N_\alpha \sigma_{ij,j}\,dv = 0. \tag{12}$$

Integration by parts of the second integral in equation (12) and the use of equation (3) gives us

$$\int_v \rho N_\alpha u_{i,t}\,dv + \int_v N_{\alpha,j}\sigma'_{ij}\,dv + \int_v N_{\alpha,j} p\delta_{ij}\,dv - \int_{S_t} N_\alpha v_j T_i\,ds = 0. \tag{13}$$

We now approximate the pressure, using the penalty function method, as

$$p = -\lambda \varepsilon_{ii}, \tag{14}$$

where λ is the penalty number. We note that the incompressible condition, equation (2), is imposed in equation (14). Substituting equations (14) and (4) into equation (13) we obtain

$$\int_v \rho N_\alpha u_{i,t}\,dv + \int_v \mu N_{\alpha,j}(u_{i,j} + u_{j,i})\,dv + \int_v \lambda N_{\alpha,j} u_{k,k}\,dv - \int_{S_t} N_\alpha v_j T_i\,ds = 0. \tag{15}$$

If now the interpolation function (11) is substituted in equation (15) we may write the equation in matrix notation as

$$[C]\{u_{i,t}\} + [K]\{u_i\} = \{F\}. \tag{16}$$

When the θ-method[7] is used for solving equation (16) we write

$$\{u_i\} = \{(1-\theta)\{u_i^t\} - \theta\{u_i^{t+\Delta t}\}\}, \tag{17}$$

$$\{u_{i,t}\} = (1/\Delta t)\{\{u_i^{t+\Delta t}\} - \{u_i^t\}\}, \tag{18}$$

where u_i^t and $u_i^{t+\Delta t}$ are the velocity at time t and $t+\Delta t$ respectively, with Δt the time interval. Equation (16) can therefore be written as

$$(1/\Delta t)[C]\{\{u_i^{t+\Delta t}\} - \{u_i^t\}\} + [K]\{(1-\theta)\{u_i^t\} + \theta\{u_i^{t+\Delta t}\}\} = \{(1-\theta)\{F_i^t\} + \theta\{F_i^{t+\Delta t}\}\}, \tag{19}$$

and rearranging we obtain

$$([C]/\Delta t + \theta[K])\{\Delta u_i^t\} = \{F\}_{\text{ave}} - [K]\{u_i^t\}, \tag{20}$$

$$u_i^{t+\Delta t} = u_i^t + \Delta u_i^t, \tag{21}$$

$$\{F\}_{\text{ave}} = \{(1-\theta)\{F_i^t\} + \theta\{F_i^{t+\Delta t}\}\}, \tag{22}$$

where $[C]$, $[K]$ and $\{F\}$ represent the coefficients from the first integral in equation (15), from the second and third integrals and from the fourth integral respectively.

A four-node rectangular isoparametric element is used for approximating the velocity. For this approximation the 2×2 Gauss–Legendre integration rule has been employed except for the third integral in equation (15). The third term, which involves the penalty number, is integrated with the one-point rule.

3.2. Marker particles for fluid motions

In order to determine the moving free surfaces, marker particles in a linear triangular element are introduced into a four-node velocity element. Figure 1(a) shows the marker in a rectangular element R0 and the eight elements around R0. We now divide the element R0 into four triangular elements and assume the marker to be in a T1 element for illustrative purposes as shown in Figure 1(b). Consider the marker in a T1 element at time t with velocity u_i and position x_i1. The position of the marker x_i2 at the next time step $t+\Delta t$ may be obtained by the equation

$$x_i2 = x_i1 + \int_t^{t+\Delta t} u_i(x_i, t)\,dt, \tag{23}$$

in which the velocity u_i of the particle can be determined by the equations

$$u_i(x_i, t) = \sum_{k=1}^{3} \xi_k u_k, \tag{24}$$

$$\xi_k = (A_k + a_i x_i 1)/2A, \tag{25}$$

where ξ_k is the area co-ordinate of the triangular element, u_k is the velocity at the kth node and A, A_k, a_i are constants calculated from the shape of triangular element.[3]

For determining the movement of the marker from element to element, we consider the marker particle to take a position in any of the five zones shown in Figure 1(c) at the very beginning of its movement. To find its earlier position within any of the five zones, we divide our time step Δt in equation (21) into n equal intervals. Next the position found is transformed into that in the area co-ordinate system. The new marker position at time $\Delta t/n$ is then determined according to the relationship between ξ_k and the sign of the area co-ordinate as shown in Table I. When the marker position is found in the next zone, we consider it as zone 0 and calculate the new marker velocity based on the triangular node velocities in zone 0. This process is continued until the step $t+\Delta t$ is completed. The interval of $\Delta t/n$ helps not only to find the new zone but also to move the marker along a streamline with better accuracy. It should be noted that the extra storage necessary to move the marker particle is that for the four elements R1, R3, R5 and R7 adjacent to element R0.

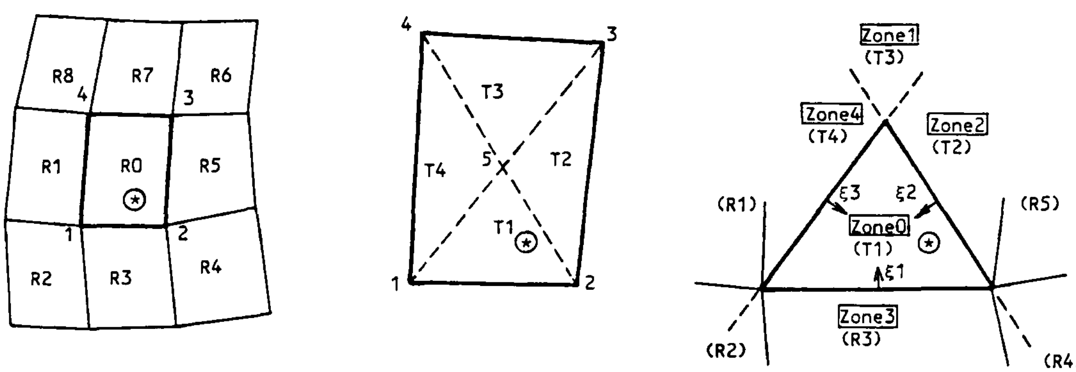

a) rectangular elements around R0 b) triangular elements in R0 c) area coordinates in T1

⊛ marker particle in T1

Figure 1. Triangular elements in a four-node element

3.3. Assumption of boundary condition and free surface

In order to proceed with the transient analysis, we assume that the free surface, which is physically a line consisting of the forefront markers and also the place to specify the boundary conditions, is located on the boundary line between the element having a forefront marker(s) and the element having not. It should be noted that the traction force along the side is zero if we do not specify any boundary values and the assumption does not affect the visualization of the free surface as a marker front.

4. EXAMPLE PROBLEMS

4.1. A punch indentation problem

In order to test the above algorithm, we first solve the Newtonian fluid flow indented by a punch. Figure 2 shows the geometry, the finite element mesh, the initial marker configuration and the results obtained by the present method. The material properties used in the analysis were $\rho = 1{\cdot}0$, $\mu = 10{\cdot}0$ and $V_0 = 1{\cdot}0$. For the analysis we chose θ in equation (16) as 0·75 from the numerical experiment to prevent the growth of wiggles in the solution. Figure 3 shows the

Table I. The five zones for marker movements

	Zone 0	Zone 1	Zone 2	Zone 3	Zone 4
ξ_1	$\geqslant 0$			< 0	
ξ_2	$\geqslant 0$	< 0	< 0	$\geqslant 0$	$\geqslant 0$
ξ_3	$\geqslant 0$	< 0	$\geqslant 0$	$\geqslant 0$	< 0

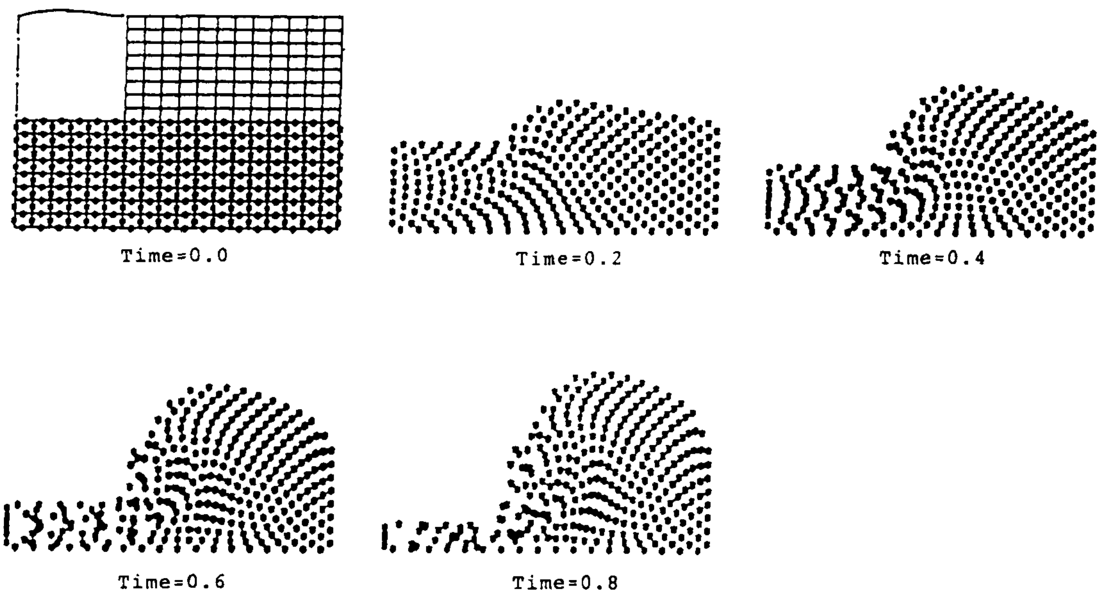

Figure 2. Punch indentation problem by the present method

calculated results obtained by the mesh-rezoning method.[1] Both the mesh-rezoning and the present method give almost identical results on the shape of the free surfaces without any difficulty. The highest swell positions at several time steps obtained by either of the methods are shown in Table II. It is interesting to note that the flow pattern of the fluid can be visualized by the present method.

4.2. *L-shaped cavity flows*

As a practical example problem, the injection moulding of an L-shaped cavity is analysed. Both Newtonian and power-law fluids are considered. The geometry and the finite element mesh used in the analysis are shown in Figure 4. The element is assumed to be filled with fluid if the marker has passed it once. This assumption requires fewer particles to be arranged in the domain and saves on computing time. With this assumption we arrange finer meshes along the walls and also arrange plenty of markers to describe the flow pattern. Along the entrance AB, 42 markers are arranged during the first $3\Delta t$ ($\Delta t = 0{\cdot}0025$ s) time period. Following that time, we place another marker in element H whenever the old marker in that element has gone. When the fluid arrives at

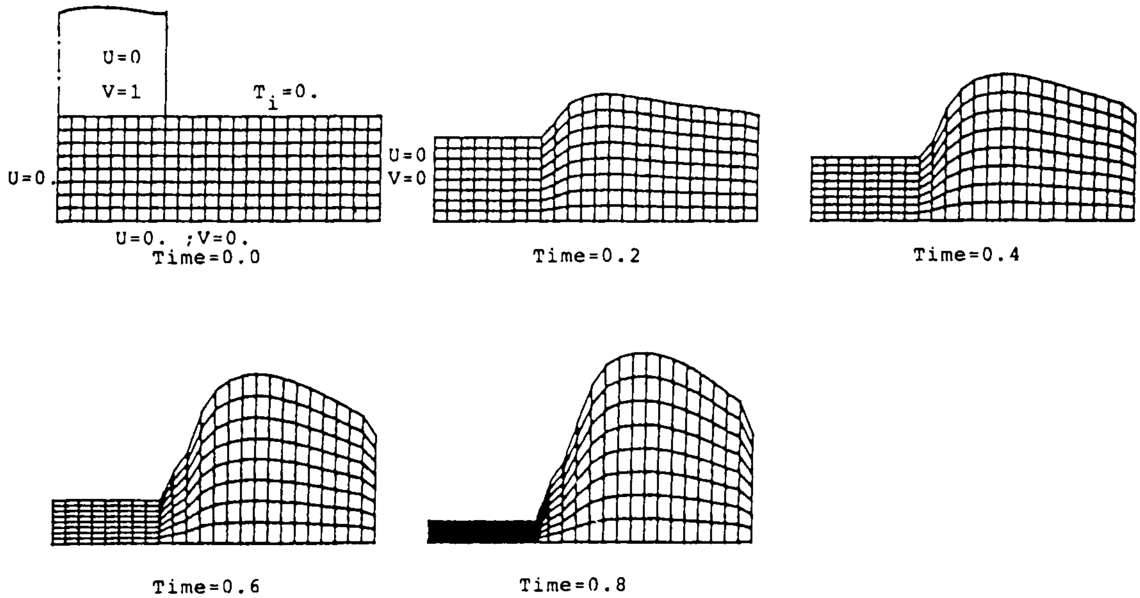

Figure 3. Punch indentation problem by mesh rezoning

Table II. Highest swell positions obtained by present method and by mesh rezoning (punch indentation problem)

	Method			
	Present		Rezoning	
Time	$\bar{x}$	$\bar{y}$	$\bar{x}$	$\bar{y}$
0·2	1·52	1·20	1·63	1·21
0·4	1·77	1·36	1·75	1·39
0·6	1·84	1·51	1·88	1·58
0·8	1·96	1·71	2·00	1·77

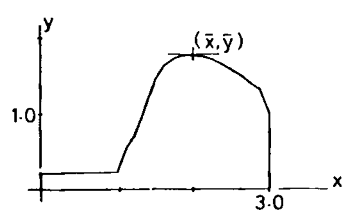

the corner F, the arranged markers are not sufficient to describe the free surface. We then add a new marker in element G at every Δt time step after the fluid passes that element.

The material properties and the specified velocity at the entrance of the cavity used here are

$$\rho = 0{\cdot}765\ \mathrm{g\,cm^{-3}},$$

Newtonian fluid

$$\mu = 3{\cdot}11 \times 10^2\ \mathrm{P},$$

$$u_{AB} = 7{\cdot}77 \times [1-(y/0{\cdot}15)^2]\ \mathrm{cm\,s^{-1}},$$

power-law fluid

$$\mu_0 = 2{\cdot}69 \times 10^3\ \mathrm{Pa\,s}^{n-1}, \quad n = 0{\cdot}467 \quad \text{when } \gamma \geqslant 0{\cdot}5,$$

$$\mu_0 = 4{\cdot}98 \times 10^3\ \mathrm{Pa\,s}^{n-1}, \quad n = 1{\cdot}000 \quad \text{when } \gamma < 0{\cdot}5,$$

$$u_{AB} = u_{max} \times [1-(y/0{\cdot}15)^{n+1/n}]\ \mathrm{cm\,s^{-1}},$$

$$u_{max} = 5{\cdot}8275 \times (2n+1)/(n+1)\ \mathrm{cm\,s^{-1}},$$

where γ is the shear strain rate.

Figures 5 and 6 show the results obtained for the Newtonian and power-law fluids respectively.

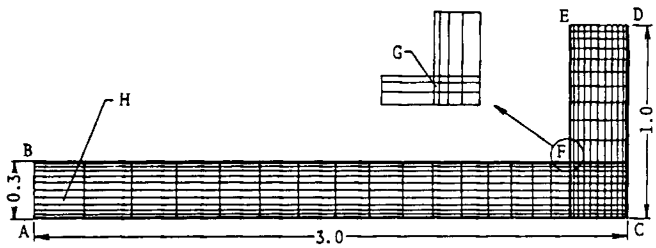

Figure 4. L-shaped cavity problem

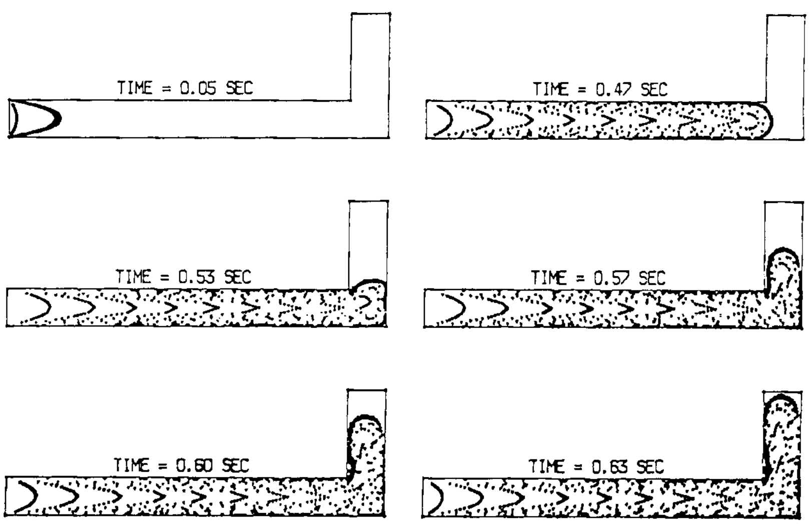

Figure 5. L-shaped cavity flow (Newtonian fluid)

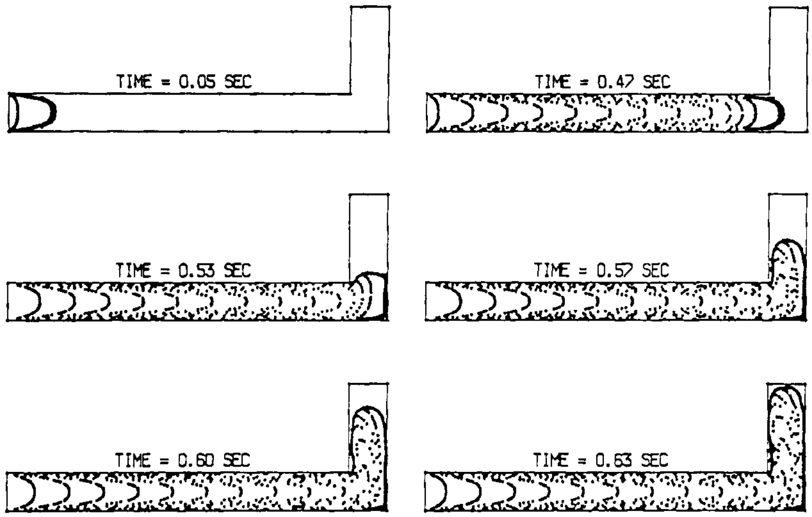

Figure 6. L-shaped cavity flow (power-law fluid)

5. CONCLUSIONS

Using the marker particle, the analysis of transient creeping flows with free surfaces by the penalty function formulation of the finite element method was described. With the present method, the free surfaces can be well simulated and the flow patterns inside of the fluid can be visualized. It should be noted that the present method is able to be applied to the problems with complicated fix-boundary conditions, which are intractable by the finite difference mehtod.

REFERENCES

1. O. C. Zienkiewicz and P. N. Godbole, 'Penalty function approach to problems of plastic flow of metal with large deformations', *J. Strain Anal.*, **10**, 180–183 (1975).
2. J. K. Dukowics, 'Conservative rezoning (remapping) for general quadrilateral meshes', *J. Comput. Phys.*, **54**, 411–424 (1984).
3. J. J. Conner and C. A. Brebbia, *Finite Element Techniques for Fluid Flow*, Butterworth, 1976.
4. B. D. Nichols and C. W. Hirt, 'Improved free surface boundary conditions for numerical incompressible-flow calculations', *J. Comput. Phys.*, **8**, 434–448 (1971).
5. F. H. Harlow, 'The particle-in-cell computing method for fluid dynamics', *Methods Comput. Phys.*, **3**, 319–343 (1964).
6. T. J. R. Hughes, W. K. Liu and A. Brooks, 'Finite element analysis in incompressible viscous flows by the penalty function formulation', *J. Comput. Phys.*, **30**, 1–60 (1979).
7. O. C. Zienkiewicz, *The Finite Element Method*, 3rd Edn, McGraw-Hill, New York, 1977.